Available online at www.sciencedirect.com
ScienceDirect
Planetary and Space Science 55 (2007) 494–502
Planetary and Space Science
www.elsevier.com/locate/pss

The D-CIXS X-ray spectrometer on the SMART-1 mission to the Moon—First results

M. Grande[a,b,*], B.J. Kellett[b], C. Howe[b], C.H. Perry[b], B. Swinyard[b], S. Dunkin[b], J. Huovelin[c], L. Alha[c], L.C. D'Uston[d], S. Maurice[d], O. Gasnault[d], S. Couturier-Doux[d], S. Barabash[e], K.H. Joy[b,f], I.A. Crawford[f], D. Lawrence[g], V. Fernandes[h], I. Casanova[i], M. Wieczorek[j], N. Thomas[k], U. Mall[l], B. Foing[m], D. Hughes[n], H. Alleyne[n], S. Russell[o], M. Grady[o], R. Lundin[h], D. Baker[p], C.D. Murray[q], J. Guest[f], A. Christou[r]

[a]*Institute of Mathematical and Physical Sciences, University of Wales, Aberystwyth Penglais, Aberystwyth, Ceredigion, SY23 3BZ, Wales. UK*
[b]*Planets and Space Plasma Group, Rutherford Appleton Laboratory, Chilton, Didcot, Oxon OX11 0QX, UK*
[c]*University of Helsinki Observatory, Finland*
[d]*CESR, CNRS/UPS, France*
[e]*IRF, Kiruna, Sweden*
[f]*UCL-Birkbeck, London, UK*
[g]*Los Alamos National Laboratory, USA*
[h]*University of Coimbra, Portugal*
[i]*UPC, Barcelona, Spain*
[j]*Institut de Physique du Globe de Paris, France*
[k]*University of Bern, Swizerland*
[l]*MPAE, Lindau, Germany*
[m]*ESTEC, Netherlands*
[n]*Sheffield University, UK*
[o]*Natural History Museum, UK*
[p]*LASP, Colorado University, USA*
[q]*QMUL, London, UK*
[r]*Queens Armagh University, UK*

Received 12 December 2005; received in revised form 4 August 2006; accepted 19 August 2006
Available online 17 January 2007

Abstract

The SMART-1 mission has recently arrived at the Moon. Its payload includes D-CIXS, a compact X-ray spectrometer. SMART-1 is a technology evaluation mission, and D-CIXS is the first of a new generation of planetary X-ray spectrometers. Novel technologies enable new capabilities for measuring the fluorescent yield of a planetary surface or atmosphere which is illuminated by solar X-rays. During the extended SMART-1 cruise phase, observations of the Earth showed strong argon emission, providing a good source for calibration and demonstrating the potential of the technique. At the Moon, our initial observations over Mare Crisium show a first unambiguous remote sensing of calcium in the lunar regolith. Data obtained are broadly consistent with current understanding of mare and highland composition. Ground truth is provided by the returned Luna 20 and 24 sample sets.

Keywords: Moon; X-ray; Composition

1. Introduction

The ESA SMART-1 mission to the Moon has recently begun science data acquisition. A major payload element is

*Corresponding author. Tel.: +44 1970 622624; fax: +44 1970 622826.
E-mail addresses: M.Grande@rl.ac.uk, M.Grande@aber.ac.uk (M. Grande).

0032-0633/$ - see front matter © 2006 Elsevier Ltd. All rights reserved.
doi:10.1016/j.pss.2006.08.004

the Demonstration of a Compact X-ray Spectrometer (D-CIXS) (Grande et al., 2002, 2003; Dunkin et al., 2003; Grande, 2001). D-CIXS is intended to provide spectroscopic mapping of the lunar surface in the X-ray range. Presented here are first observations of the Earth and Moon using the D-CIXS spectrometer.

The Apollo 15 and 16 and the NEAR mission to asteroid Eros all carried simple X-ray fluorescence instruments (Adler et al., 1972; Goldsten et al., 1997). These instruments consisted of three sealed proportional counter X-ray detectors of 25 cm^2 area—one detector was left with just a beryllium window, a second detector had an additional aluminium filter and the third detector a magnesium filter. At low X-ray energies, the main rock-forming elements (Mg, Al and Si) produce three lines between 1 and 2 keV. The magnesium filter was designed to completely remove the aluminium and silicon lines and leave the magnesium line untouched. The thick aluminium filter was designed to just remove the silicon line and leave the magnesium and aluminium lines untouched. Therefore, with three such detectors it is possible to isolate the flux from the Mg, Al, and Si fluorescence lines (but this flux will also include a contribution from the scattered solar continuum spectrum). The Apollo instruments possessed essentially no intrinsic energy resolution while the NEAR Shoemaker detectors had an energy resolution of ~900 eV at 5.9 keV (15%—Goldsten et al., 1997). However, the Mg, Al and Si lines are only ~250 eV apart, so the NEAR Shoemaker X-ray spectrometer relies on the same Apollo-style filter ratio technique to isolate these elements/lines. The NEAR Shoemaker experiment also carried a similar gas counter and also a Si PIN diode as solar spectrum monitors. The Si PIN diode had an energy resolution of ~600 eV (Goldsten et al., 1997).

D-CIXS demonstrates a new approach to building this type of X-ray spectrometer. This is the first time that electronic solid-state detectors have been used for this purpose. It requires a resource envelope far smaller than earlier instruments of this kind, using new technology which does not require cooling of the detector plane, and hence greatly reduces the overheads to the spacecraft. It consists of a high throughput spectrometer, which performs spatially localised X-ray fluorescence spectroscopy; a solar monitor provides calibration which is necessary for producing absolute lunar elemental abundances. A relatively large collecting area and angular acceptance is essential at the Moon, which is a very weak source, particularly during the current solar minimum epoch. D-CIXS can derive 42 km spatial resolution on the lunar surface from a 300 km orbiting spacecraft, although in general its resolution is limited by the number of X-ray photons available from the given solar illumination. A more complete description of the instrument is given in Grande et al., 2003.

The essential concept of the instrument is a thin, low profile detector, centring on the use of a dual microstructure collimator and swept charge device (SCDs) detectors. The advanced low-profile microstructure collimation and filter design builds on expertise developed in solid state and microwave technology to enable us to dramatically reduce the instrument mass. It is based on a new negative photoresist exposed using ultraviolet radiation. This photoresist has been designed for very thick layers and has good mechanical properties and can be used to produce features that have high aspect ratios and sidewall angles approaching 90°. The sidewalls are sufficiently rough to provide collimation.

SCD detectors are a novel architecture based on proven CCD technology. They have the virtue of providing good X-ray detection and spectroscopic measurement capabilities, while also operating at ambient temperature. Thus, we avoid the need for the large passive cooling radiator that is generally required to cool large X-ray focal plane CCDs. The devices are manufactured on high resistivity silicon, with supplementary 'narrow' channels to increase radiation tolerance. D-CIXS has 24 such detectors, providing an effective area of 14 cm^2 at 1–2 keV. These are grouped in three facets of eight detectors. The central nadir-pointing facet (facet 2) has a field of view of 8°, while the two outer facets (1 and 3) have fields of 12° and are offset from nadir by ±10°. Facets 1 and 2 have filters comprising a 4000 Å layer of aluminium on a 4000 Å polyimide substrate, to remove UV and low-energy particle backgrounds while not appreciably attenuating X-ray energies above 0.7 keV. Facet 3 has a 6 μm magnesium filter (as well as 7000 Å of polyamide and 600 Å of aluminium) and so is essentially only sensitive to magnesium fluorescence in the low energy region. The energy range of interest is 0.7–7 keV with an energy resolution sufficient to separate elemental lines. This is all achieved in a mass of only ~4.5 kg. For comparison, the NEAR X-ray instrument weighed around 21 kg in total.

The D-CIXS baseline specification requires that:

- It can measure the absolute abundances of the major rock-forming elements Mg, Al, Si, Ca, Fe and others. Al/Mg and Al/Si ratio maps have been proved to be particularly useful for discriminating between different lunar surface materials (Adler et al., 1972; Adler and Trombka, 1977; Clark and Adler, 1978; Bielefeld, 1977; Andre et al., 1978).
- It has a large effective aperture, at least the 14 cm^2 needed to obtain statistically meaningful results from an extremely weak signal.
- It can provide measurement of abundances at the lunar surface with a spatial resolution of the order of 50 km for the low energy lines for a 300 km spacecraft altitude.
- It has sufficient spectral resolution to be able to distinguish the relatively close lines of Mg, Al and Si at the low-energy end of the spectrum. At launch the resolution was better than 250 eV, and after the long cruise through the Earth's radiation belts and interplanetary space, is currently around 380 eV. This is sufficient for elemental analysis. We currently anticipate

an anneal cycle to improve detector resolution at the start of the extended mission.

- It simultaneously monitors the solar X-ray flux, utilising the X-ray solar monitor (XSM) (Huovelin et al., 2001) in order to obtain absolute surface abundance measurements.

2. Observations of terrestrial argon

The SMART-1 mission was launched on 27 September 2003. The ion propulsion engine of SMART-1 took around 15 months to reach lunar orbit. The first ~6 months and the final ~3 months of this period were reserved for spacecraft propulsion operations, but the intervening ~6 months were available for so called "cruise" observations of the Earth and selected astronomical targets. So, on 16 July 2004, while performing a routine observation of the Earth with the AMIE camera (Pinet et al., 2005), we had an opportunity to demonstrate the viability of the technique by observing fluorescence from the Earth. The observation was only about 2 h long but during this period an X-class solar flare occurred. The time evolution, as measured by the NOAA GOES-10 Space Environment Monitor, is shown in Fig. 1(b). Throughout this paper, we have used the GOES X-ray data to illustrate the context of the D-CIXS, since the GOES data form a continuous, unbroken data series during this epoch. GOES measures the solar X-ray flux in a soft (1–8 Å) and hard (0.5–3 Å) energy band. For every increase of a factor of ten in the soft flux, a different letter is assigned from A for the lowest flux band through B, C, M and final X-band–a factor of 10,000 in flux above the A band. Fig. 1(b) also shows the simultaneous X-ray response from the Earth as detected by D-CIXS. The very similar response indicates that we are indeed seeing X-ray fluorescence. Data were taken from the eight detectors of the instrument (centre facet/facet 2) which were pointing towards the Earth. The central energy of the peak generated from this observation is situated at 2.89 keV, which is very close to the expected Argon Kα line at 2.958 keV (Table 1). The is within one energy channel (~67 eV), indicating that the calibration has changed little from the ground derived values. The average estimated full width at half maximum (FWHM) is of order 380 eV, substantially larger than the values derived from a calibration source shortly after launch. This broadening of the energy response is ascribed to the heavy dose of penetrating particle radiation during the early phases of the mission, when the ion propulsion of the spacecraft was used to slowly raise the altitude of the orbit through the radiation belts.

X-ray observations of the Earth are fairly rare. However, the NASA/GGS satellite POLAR did carry PIXIE, a simple X-ray pinhole camera and gas proportional counter detector system (Petrinec et al., 2000). This instrument provided images but the spectral energy resolution of the gas detector is limited. In the latter part of 1998, PIXIE observed the signatures of several large solar X-ray flares. The X-ray spectra included the Thompson scattered solar X-ray spectrum and argon fluorescence (Petrinec et al.,

Table 1
Derived responses for the eight detectors in facet 2 (centre facet)

Detector	SiO layer (Å)	Al layer (Å)	Efficiency	Line centre (keV)	Line FWHM (eV)
1	5500	4063	0.62	2.83	353
2	2000	3750	0.48	2.99	308
3	2500	7031	0.71	2.89	260
4	3875	5313	0.62	2.90	364
5	3625	5938	0.66	2.92	335
6	4375	4219	0.40	2.76	422
7	3000	5938	0.53	2.77	484
8	5125	5313	0.48	2.92	348

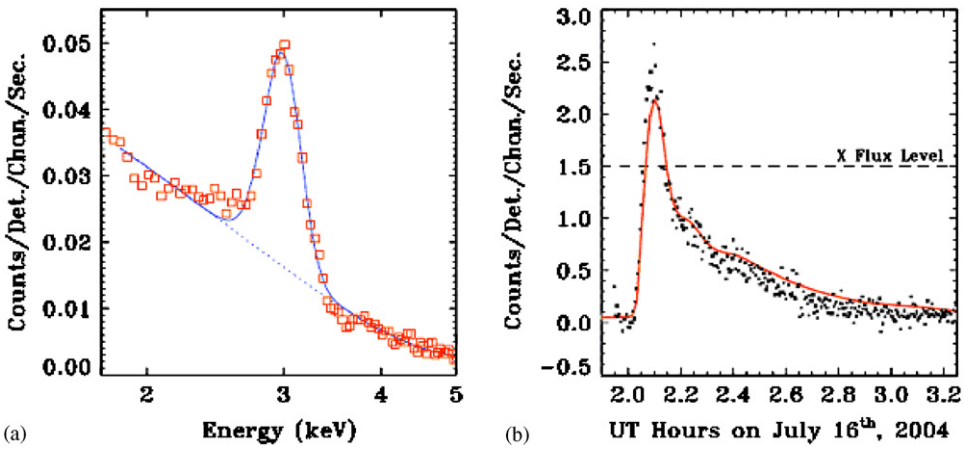

Fig. 1. (a) The integrated spectrum from the centre facet (facet 2) with the argon line at 2.96 keV, and with the fitted background and line indicated. (b) The integrated signal from the earth (squares) compared with the solar X-ray emission observed by GOES (solid line) during the flare event. (The GOES X flare level is indicated by the dashed line).

2000). However, the argon line is not easily seen in the published spectrum and its presence is only determined by detailed analytical modelling. In a forthcoming paper (Kellett et al., in preparation). we will provide detailed analysis of the two X-ray flares D-CIXS detected at Earth.

3. Calibration

During the cruise phase, the detectors in the centre facet (facet 2) of the instrument were calibrated using the Crab nebula, a well-characterised X-ray source (Kirsch et al., 2005), which was observed for approximately 2 h on October 5, 2005 between 16:32 and 18:33 (UT). After the removal of noisy spectral data, good spectra in all detectors were co-added. All spectra were interpolated onto a single energy scale using the original ground-based calibrations. The constant particle background was estimated using data acquired with the adjacent facet which had been observing empty space. The measured spectra were divided by the expected

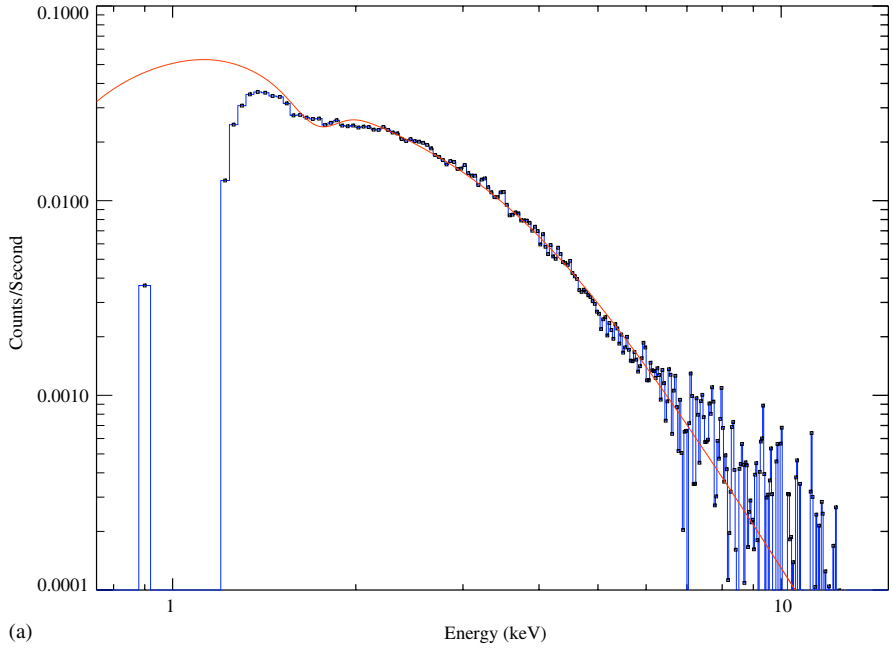

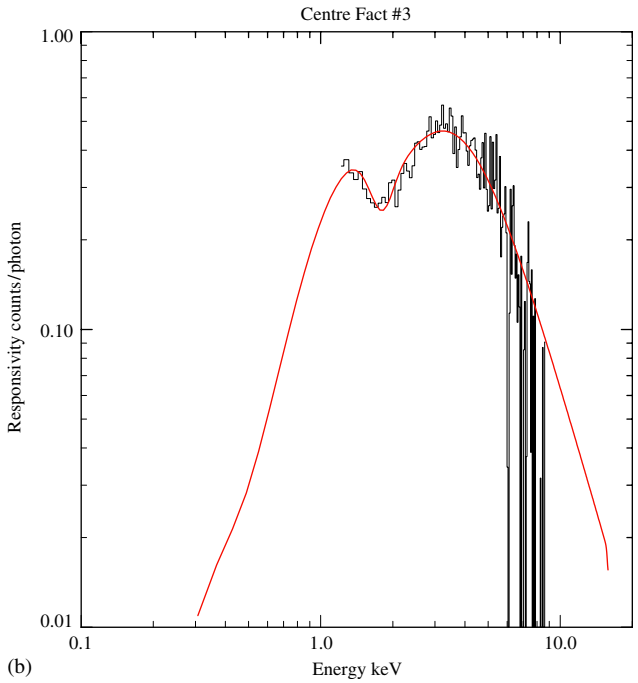

Fig. 2. (a) A comparison of observed (histogram) and modelled (line) Crab spectra The reference spectrum of Kirsch et al., 2005 is used in the model. (b) Measured and fitted instrument relative response curves for central facet.

spectrum to give the instrument response in units of counts cm^2/photon i.e. the instrument relative response function. This measured response is compared with a "model" instrument response based on the assumption of 100% efficient silicon detectors with an absorption layer of 14 μm covered with a carbon filter substrate of 4000 Å, an aluminium filter layer of 4000 Å and a non-sensitive passive layer of silicon dioxide of 4000 Å thickness on the front of the detector. The FWHM of detector response was taken to be 380 eV. These parameters were varied iteratively to derive the measured responses for the individual detectors (Table 1). The model and observed spectra are shown in Fig. 2a and b shows the derived response function. Similar calibrations of the two side facets await calibration from observations of the Crab, and this will be carried out during the extended mission. Instrumental efficiencies have been corrected for the known factor 0.29 obscuration of the collimators. The average efficiency relative to the ideal is 56%. Fuller descriptions of analysis and calibration procedures form the subject of further projected publications.

4. Observations of Mare Crisium

In March 2005, the SMART-1 spacecraft reached its nominal lunar orbit, and we began full commissioning for lunar operations. During the pre-commissioning period in mid-January 2005, observations of the lunar surface were made which coincided with the occurrence of several major M- and X-class flares. This opportunity provided an excellent chance to observe spatially localised fluorescence from the lunar surface. Data obtained by D-CIXS and the XSM for the full interval of four flares in mid-January is shown in Fig. 3. X-ray fluorescent elemental lines from the lunar surface are detected by all three facets of D-CIXS while the XSM instrument observes the input solar spectrum.

At the end of this interval, a long duration M-class solar flare began at 06:00 UTC on 15 January 2005 (Fig. 3). The flare lasted for more than 1 h but only ~30 min corresponded to D-CIXS observations. At this time, SMART-1 was orbiting over the Moon's near-side eastern limb from about the equator, travelling northwards (Fig. 4). As SMART-1 flew north, its altitude was also increasing from

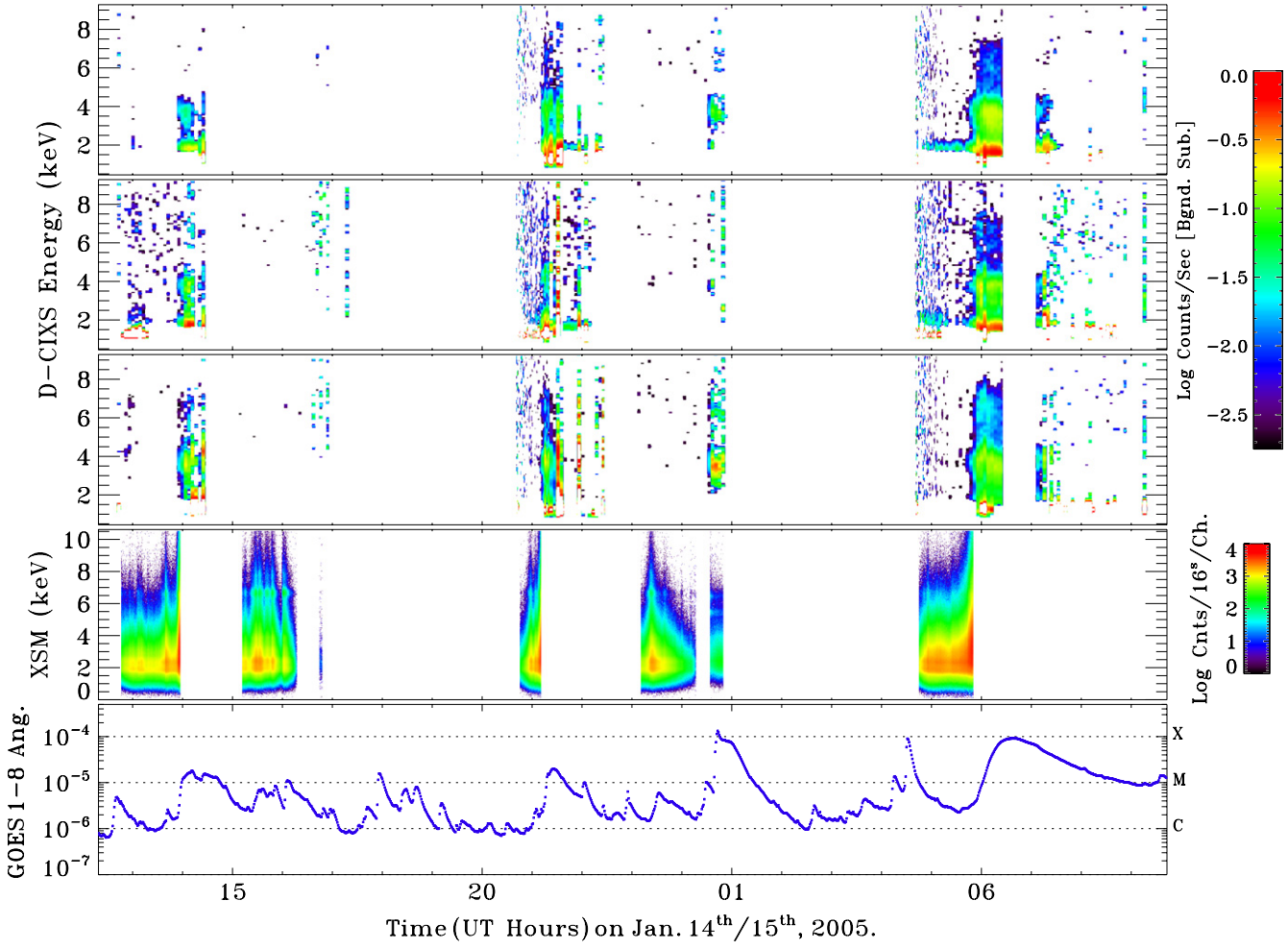

Fig. 3. Total X-ray counts from each facet of DCIXS (panels 1–3) and XSM (panel 4). Data from GOES are shown (in units of W/m^{-2}) for comparison purposes in the bottom panel with the C- M- and X-flare levels indicated.

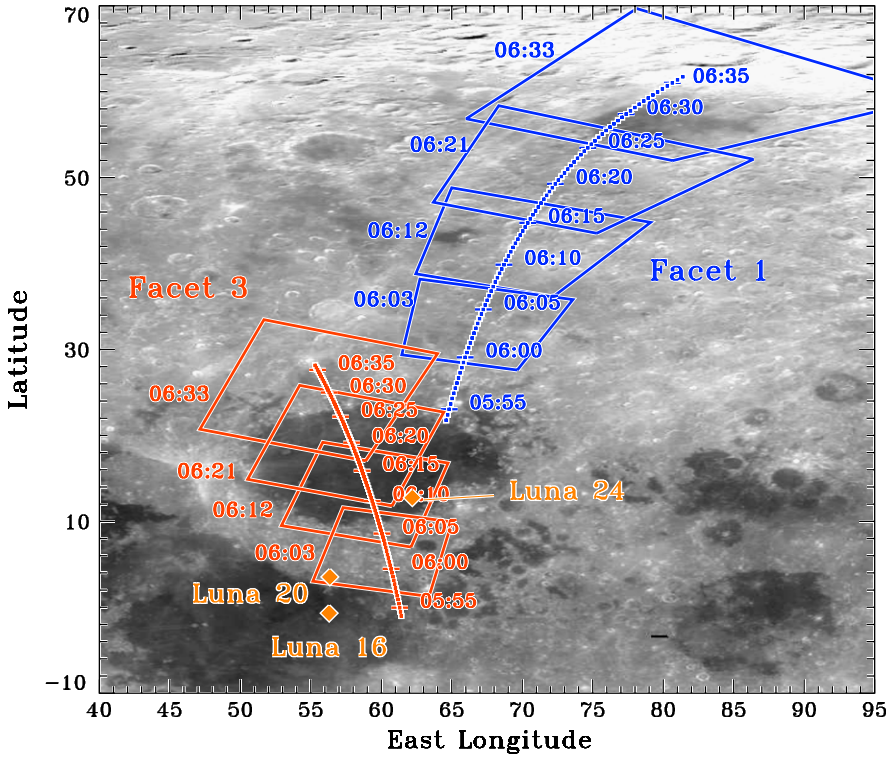

Fig. 4. Groundtracks of D-CIXS's facets 1 and 3 superimposed on the areas of the Moon overflown during the January 15, 2005 flare observation. The squares indicate the FWHM of the field-of-view of the detectors at the given times. The centre track of each facet is also shown, along with the landing sites of the three Soviet Luna robotic landers. Underlying map is from USGS/PDS based on Clementine 710 nm data and has been contrast enhanced.

around 2100 km at 06:00–~3100 km at 06:35. Due to the nature of SMART-1's orbit and thermal dynamics, the spacecraft was performing a mid-orbit slew (rotation), and so D-CIXS's three facets had different surface groundtracks during the observation of interest (Fig. 4). However, this variability in footprints was very fortuitous as the instrument FOVs included areas of both mare basalt and highland lithologies, which have different and recognisable elemental signatures. Facet 1 (thin Al-filter, 12° FOV) was oriented throughout the observation toward highland areas to the north-east of Mare Crisium. Facet 3 (Mg-filter, 12° FOV) had a groundtrack that crossed Mare Crisium. Due to the 12° FOV and the 2100 km altitude, the facet 3 footprint always contains a mixture of mare and highland regions. The footprint of facet 2 (thin Al-filter, 8° FOV) (not shown) encompassed the regions between the two facets shown and covered a mixture of mare and highland regions but with a smaller signal due to its narrower FOV.

Preliminary science data processing, using the same techniques used to analyse Earth observation data, has been undertaken on this D-CIXS lunar flare data. Fig. 5 shows the particle background corrected spectra from summed data of the 3 D-CIXS facets for the interval 06:00 UTC to 06:35 UTC. Separate facet spectra have been derived by co-adding data from detectors. Essentially, elemental lines seen in the three different facet spectra represent an averaged geochemical signature from the areas covered by the D-CIXS groundtracks (Fig. 4).

The spectra shown in Fig. 5 indicate that low-energy lines (Mg: 1.25 keV, Al; 1.49 keV and Si: 1.74 keV) are observed in detectors from facets 1 and 2 (Al-filter). Detectors in facet 3 are covered by a magnesium filter which was designed to attenuate the signal from Al and Si X-rays, and so in the facet 3 spectrum Mg is the only significant low-energy peak detected. Data taken from the facet 3 spectrum also show a clear Fe peak at around 6.4 keV which is interpreted to be related to fluorescence from Mare Crisium (see below). All three facets clearly show the detection of a Ca emission peak at ~3.69 keV. Although inferences about the distribution of Ca in the lunar crust have been made indirectly from neutron and gamma ray measurements (Elphic et al., 2000; Prettyman et al., 2002), this observation represents the first ever unambiguous remote sensing of Ca on the Moon.

5. Discussion

Fig. 6 shows the instantaneous spectra observed in facets 1 and 3 at ~06:15 UT, when facet 1 was observing highland terrain while facet 3 was observing Mare Crisium (see Fig. 4). The same broad spectral features as those seen in the full integrated spectrum can still be clearly identified in just a ~2 min exposure.

The areas of the lunar surface observed during the flare of January 15 include Mare Crisium, and highlands to the north and east (Fig. 4). The basaltic lavas of Mare Crisium, which appear dark in Fig. 4, are iron-rich owing to high

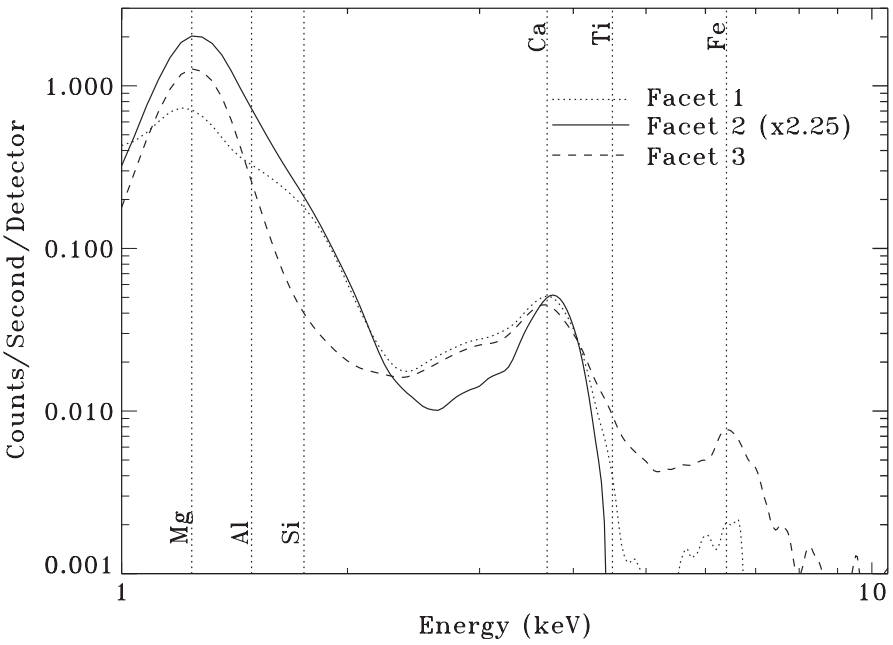

Fig. 5. Average spectra from facets 1, 2 and 3 showing the clear detection of emission from calcium and iron and a merged peak from magnesium, aluminium and silicon visible in the facets 1 and 2 spectra. Facet 3 is covered by a magnesium filter, and hence does not contain the aluminium and silicon lines visible in facets 1 and 2. Note that facet 2 has an 8 degree FOV and hence is normalised by a factor 2.25 relative to the 12 degree FOV of facets 1 and 3. The spectra are averaged over the period between 06:00 and 06:35 UT on 15 January 2005.

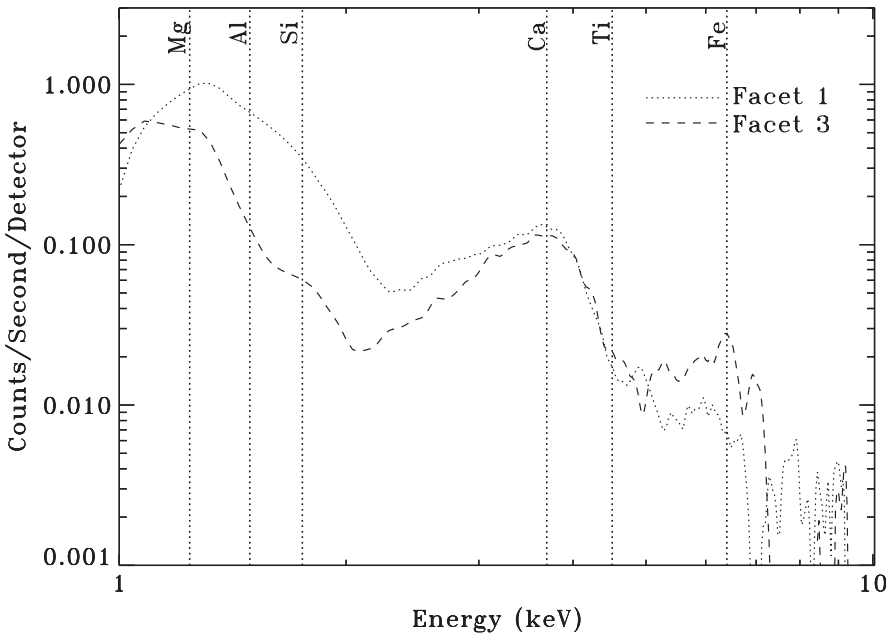

Fig. 6. Instantaneous spectra from facets 1 and 3. The spectra clearly show that emission from calcium, iron, magnesium, aluminium and silicon can still be obtained in just a ~2 min period centred at 06:15 UT when facet 3 was over the centre of Mare Crisium and facet 1 was observing the highlands north and east of Crisium. Important elements are marked by vertical dotted lines.

modal abundances of mafic minerals (principally pyroxene). In contrast, the adjacent highlands are expected to be anorthositic (i.e., composed largely of the mineral plagioclase), and thus iron poor but relatively enriched in calcium and aluminium. Some 'ground truth' is provided by samples collected at the Luna 20 and 24 landing sites, both of which were located within the footprint of facet 3 during these observations (Fig. 4). Table 2 lists the average major element concentrations (by number of atoms) in soils and regolith breccias returned from these two sites (derived from the oxide weight percentages tabulated by Haskin and Warren, 1991).

Table 2
Concentrations of major elements in Luna 20 and 24 soils and regolith breccias (after Haskin and Warren, 1991)

Element	Luna 20 (highland)		Luna 24 (Mare Crisium)	
	Wt%	At%	Wt%	At%
O	44.5	60.6	42.1	60.2
Si	21.0	16.3	21.4	17.3
Al	12.0	9.7	6.4	5.4
Ca	10.4	5.7	8.0	4.6
Fe	5.8	2.2	15.3	6.3
Mg	5.8	5.2	6.0	5.7
Na	0.3	0.3	0.2	0.2
Ti	0.3	0.1	0.6	0.3

Remote sensing by *Clementine* (e.g. Bussey and Soudis, 2000; Lucey et al., 2000) and *Lunar Prospector* (e.g. Lawrence et al., 2002) suggests that the Soviet Luna 24 and Luna 20 iron abundances are reasonably representative of the Mare Crisium basalts, and the adjacent highlands, respectively. These remote sensing data also suggest that the highlands north and east of Crisium, which have a higher albedo in Fig. 4, are more anorthositic (i.e. poorer in Fe and richer in Ca) than those immediately adjacent to the Crisium basin and which were sampled by Luna 20.

These expectations are confirmed by the D-CIXS data shown in Fig. 6, which were obtained at 06:15 UT when facet 3 was over the centre of Crisium and facet 1 was observing the highlands approximately 900 km to the north (material apparently similar to that of the highlands of the Luna 20 landing site). As expected, the Fe flux is strongly enhanced over Crisium (dashed spectrum in Fig. 6), while Ca is somewhat enhanced over the highlands (dotted spectrum in Fig. 6). Moreover, although there is strictly no ground truth available for the facet 1 footprint, the greater variability of Fe relative to Ca between mare and highland regions apparent in Fig. 6 is explicable in terms of the Luna 20 and 24 results presented in Table 2: while Fe is almost three times as abundant in the Crisium basalts than in the adjacent highlands, the Ca abundance is only some 20% less. Essentially the same trend is obtained by comparing the Fe and Ca Lunar Prospector data (Prettyman et al., 2002), which imply a factor of 2 difference in Fe, but less than a 10% difference in Ca, between these two footprints.

6. Conclusion

During the SMART-1 mission cruise phase, successful observations were made of well-known astronomical X-ray targets including the Crab nebula. Argon has also been successfully detected in the Earth's atmosphere. The instrument demonstrates the capability of this method to perform X-ray fluorescence measurements of the Moon. A number of rock forming elements have been successfully detected from the Moon during solar flare events and we have made the first unambiguous detection of Calcium from the lunar surface. All of this has been achieved during solar minimum and proves that the technique will be highly suitable for the upcoming Chandrayaan-1 mission (Grande et al., 2003), when the mission will take place during the rising phase of the solar cycle, and for which it forms part of the core payload.

Acknowledgements

Thanks to the first referee and George Fraser for helpful comments.

References

Adler, I., Trombka, J.I., 1977. Phys. Chem. Earth 10, 17.
Adler, I., 10 colleagues, 1972. Apollo 15 geochemical X-ray fluorescence experiment: preliminary report. Science 175, 436–440.
Andre, C.G., Wolfe, R.W., Andler, I., 1978. Evidence for a high-magnesium subsurface basalt in Mare Crisium from orbital X-ray flourescence data. In: Merrill, R.B., Papike, J.J. (Eds.), Mare Crisium: The View from Luna, vol. 24. Pergamon Press, Tarrytown, NY, pp. 1–12.
Bielefeld, M.J., 1977. Lunar surface chemistry of regions common to the orbital X-ray and gamma-ray experiments. In: Proceedings of the Eighth Lunar Science Conference, pp. 1131–1147.
Bussey, D.B., Soudis, P.D., 2000. Compositional studies of the Orientale, Humorum, Nectaris, and Crisium lunar basins. J. Geophys. Res.—Planets 105, 4235–4243.
Clark, P.E., Adler, I., 1978. Utilization of independent solar flux measurements to eliminate non-geochemical variation in X-ray fluorescence data. In: The Ninth Lunar and Planetary Science Conference. pp, 3029–3036.
Dunkin, S.K., et al., 2003. Scientific rationale for the D-CIXS X-ray spectrometer on board ESA's SMART-1 mission to the Moon. Planet. Space Sci. 51 (6), 435.
Elphic, R.C., Lawrence, D.J., Feldman, W.C., Barraclough, B.L., Maurice, S., Binder, A.B., Lucey, P.G., 2000. Determination of lunar global rare earth abundances using Lunar Prospector neutron spectrometer observations. J. Geophys. Res.—Planets 105 (#E8), 20333–20346.
Goldsten, J.O., 15 colleagues, 1997. The X-ray/gamma-ray spectrometer on the near earth asteroid rendezvous mission. Space Sci. Rev. 82, 169–216.
Grande, M., 2001. The D-CIXS X-ray spectrometer on ESA's SMART-1 mission to the Moon. Earth Moon Planets 85 (6), 143–152.
Grande, M., Dunkin, S., Heather, D., Kellett, B., Perry, C.H., Browning, R., Waltham, N., Parker, D., Kent, B., Swinyard, B., Fereday, J., Howe, C., Huovelin, J., Muhli, P., Hakala, P.J., Vilhu, O., Thomas, N., Hughes, D., Alleyne, H., Grady, M., Russell, S., Lundin, R., Barabash, S., Baker, D., Clark, P.E., Murray, C.D., Christou, A., Guest, J., Casanova, I., d'Uston, L.C., Maurice, S., Foing, B., Kato, M., 2002. The D-CIXS X-ray spectrometer, and its capabilities for lunar science Lunar Exploration 2000, 2002. Adv. Space Res. 30 (8), 1901–1907.
Grande, M., (+47 authors), et al., 2003. The D-CIXS X-ray mapping spectrometer on SMART-1. Planet. Space. Sci. 51 (6), 427.
Haskin, L., Warren, P., 1991. In: Heiken, G.H., Vaniman, D.T., French, B.M. (Eds.), The Lunar Sourcebook. Cambridge University Press, Cambridge, pp. 449–451.
Huovelin, J., Alha, L., Andersson, H., Andersson, T., Browning, R., Drummond, D., Foing, B., Grande, M., Hamalainen, K., Laukkanen, J., Lamsa, V., Muinonen, K., Murray, M., Nenonen, S., Salminen, A., Sipila, H., Taylor, I., Vilhu, O., Waltham, N., Lopez-Jorkama, M., 2001. The SMART-1 X-ray solar monitor (XSM): calibration for

D-CIXS and independent coronal science. Planet. Space Sci. 2002 50 (14–15), 1345–1353.

Kirsch, M.G.F., et al., 2005. Proc. SPIE 5898, 22.

Lawrence, D.J., Feldman, W.C., Elphic, R.C., Little, R.C., Prettyman, T.H., Maurice, S., Lucey, P.G., Binder, A.B., 2002. Iron abundances on the lunar surface as measured by the Lunar Prospector gamma-ray and neutron spectrometers. J. Geophys. Res.—Planets 107 (E12), 5130.

Lucey, P.G., Blewett, D.T., Jolliff, B.L., 2000. Lunar iron and titanium abundance algorithms based on final processing of Clementine ultraviolet–visible images. J. Goegr Res 105, 20297–20305.

Petrinec, S.M., McKenzie, D.L., Imhof, W.L., Mobilia, J., Chenette, D.L., 2000. Studies of X-ray observations from PIXIE. J. Atmos. Sol. Terres. Phys. 62, 875.

Pinet, P., (+18 authors), et al., 2005. The advanced Moon micro-imager experiment (AMIE) on SMART-1: scientific goals and expected results. Planet. Space Sci. 53 (13), 1309.

Prettyman, T.H., Feldman, W.C., Lawrence, D.J., McKinney, G.W., Binder, A.B., Elphic, R.C., Gasnault, O.M., Maurice, S., Moore, K.R., 2002. Library least squares analysis of Lunar Prospector gamma-ray spectra. In: The 33rd Lunar and Planetary Science Conference, Abstract 2012.